

UNCLASSIFIED

Defense Technical Information Center  
Compilation Part Notice

ADP010748

TITLE: Combined Measurements and Computations of  
High Enthalpy and Plasma Flows for Determination  
of TPM Surface Catalycity

DISTRIBUTION: Approved for public release, distribution unlimited

This paper is part of the following report:

TITLE: Measurement Techniques for High Enthalpy  
and Plasma Flows [Techniques de mesure pour les  
ecoulements de plasma et les ecoulements a haute  
enthalpie]

To order the complete compilation report, use: ADA390586

The component part is provided here to allow users access to individually authored sections of proceedings, annals, symposia, ect. However, the component should be considered within the context of the overall compilation report and not as a stand-alone technical report.

The following component part numbers comprise the compilation report:

ADP010736 thru ADP010751

UNCLASSIFIED

# Combined Measurements and Computations of High Enthalpy and Plasma Flows for Determination of TPM Surface Catalycity

A.F. Kolesnikov

Institute for Problems in Mechanics RAS  
Prospect Vernadskogo 101/1  
117526 Moscow  
Russia

## Summary

The paper presents the method for the TPM catalycity prediction on the basis of high enthalpy plasmatron heat transfer tests, performed in subsonic regimes, and appropriate CFD modeling of the whole plasma flow field in the plasma wind tunnel (1), viscous reacting gas flows around a test model (2), a nonequilibrium boundary layer near the stagnation point of a test model (3) and analysis of the the heat transfer for test conditions at the small Reynolds and Mach numbers (4). In general, the methodology was developed during the study of the catalytic efficiencies of the Buran TPM - the black ceramic tile and the C-C material with antioxidation coating - in dissociated nitrogen and air reacting flows. This experimental-theoretical methodology has been modified recently for the determination of TPM catalycity in subsonic carbon dioxide and pure oxygen flows from high enthalpy tests performed by using the 100-kW inductive IPG-4 plasmatron. The interaction between combined ground test measurements and CFD modeling is considered as genesis for catalytic effects duplication, plasma flow field rebuilding and the extraction of the quantitative catalycity parameters from the measured high enthalpy flow parameters, surface temperature and stagnation point heat fluxes.

## 1. Introduction

Apparently it was Bonhoeffer who first observed the heat effect of atoms heterogeneous recombination exposing the thermometer with bulb, covered with a thin layer of the catalyst, in the dissociated hydrogen flow [ref. 1]. The thermometer indicated different temperatures for different catalysts. More then 40 years ago Fay and Riddell [ref. 2], and Gulard [ref. 3] for the first time numerically estimated the catalysis heat effect on heat transfer from hypersonic flow to stagnation point of a blunt body.

It is well known now that surface catalysis plays a key role in the heat transfer to space vehicles with the reusable thermal protection system (TPS) such as the Space Shuttle [refs. 4-6], the Buran and Bor [refs. 7, 8]. Fig. 1 shows the calculated temperature distribution along the lower surface of the Bor vehicle for the altitude 72.4 km and velocity 6450 m/s and flight test data [ref. 8]. The temperature jump on the thermal protection tile, covered with high catalytic black platinum, reached

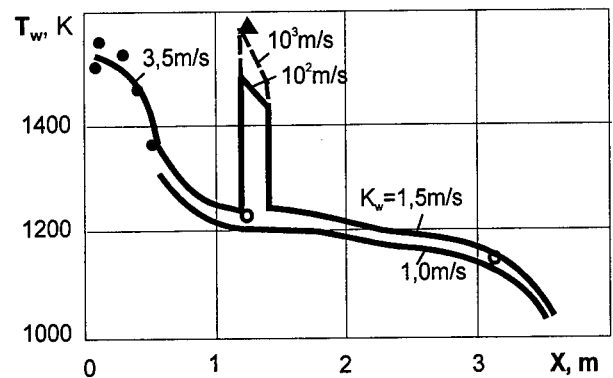


Fig. 1. Surface temperature distribution along the windward center line of the Bor vehicle [ref. 8]. Dots - the flight test data: 1 - C-C material with antioxidation coating; 2 - ceramic tile; 3 - ceramic tile covered with black platinum. Curves - computations at different catalytic recombination rates  $K_w$ .

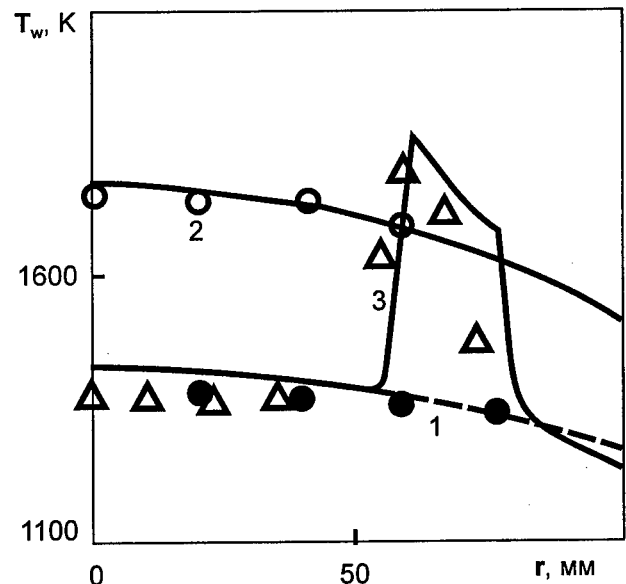


Fig. 2. Effect of the "overequilibrium" heating of the ceramic tile with nonuniform catalytic coating [ref. 9]. Dots - test in subsonic air flow at the pressure 0.015 atm, enthalpy 23.5 MJ/kg, velocity 650 m/s: 1 - clean tile, 2 - tile fully covered with spinel, 3 - tile with a high-catalytic spot (nickel-chrome spinel ring). Curves - numerical solution of Navier-Stokes equations for nonequilibrium dissociated nitrogen: 1 -  $K_{wN}=1$  m/s, 2 -  $c_{wN}=0$ , 3 - surface with a discontinuity of catalycity.

almost 400 K. Similar effects of the high catalytic spots "overheating" were observed before in the flight experiment on the Space Shuttle [ref. 5] and in ground test performed in the 1-MW IPG-3 plasmatron (IPM) in subsonic high enthalpy air flow [ref. 9] (see Fig. 2).

Surface catalysis may contribute essentially in heat transfer to a vehicle surface during a hypersonic entry into the Martian atmosphere. According to calculations [refs. 10, 11], the predicted stagnation point heat fluxes to the Mars Pathfinder aeroshell and Mars Probe are 3 times greater for the case of a fully catalytic surface in comparison with a noncatalytic surface case for the peak-heating points of the entry trajectories.

It is necessary to understand that surface catalycity can not be measured directly in an experiment. The catalytic recombination of atoms at the TPM surface has complex poorly-defined kinetics which include the following processes [ref. 12]:

- activation and deactivation of the surface sites;
- atoms adsorption and desorption:  $A+S \leftrightarrow A_S$ ;
- adatoms  $A_S$  surface migration;
- catalytic recombination of atoms through Eley-Rideal mechanism  $A+A_S \rightarrow A_2+S$  and Langmuir-Hinshelwood mechanism  $A_S+A_S \rightarrow A_2+2S$ ;
- formation and quenching of excited molecules.

No theories yet exist to predict the TPM catalycity beyond experiment. The only answer is to determine effective catalytic properties of the TPM from the ground test and to extrapolate accurately to flight conditions [ref. 13].

The method of the inductive heating of gases revealed the efficient way of the production of the unpolluted plasma flows with a temperature level close to gas temperatures at the outer edge of boundary layer at a blunt body when it moves in atmosphere at a hypersonic velocity [refs. 14-16]. This feature combined with a high stability of inductive coupled plasmas provided a basis for the development of the inductive plasmatrons [refs. 17-24] for the studies of the high-enthalpy flows, TPM testing, and real gas effects and plasma/surface interaction, including the contribution of the catalytic effects in surface heating.

The plasmatrons of the IPG family at IPM RAS appeared to be very efficient tools for the ablative TPM samples testing [ref. 25], and the prediction of the TPM catalycity, the testing of the full-scale TPS elements and the studies of TPM behavior in high enthalpy air flows in the course of the Buran program in 1978-1988 [refs. 9, 17, 18, 26, 27]. The efficient capabilities of the 100-kW IPG-4 plasmatron for the simulation of physico-chemical processes accompanying the hypersonic entry of a vehicle aeroshell in the Martian atmosphere have been demonstrated recently [refs. 24, 28-30].

This paper is focused on the method for the TPM catalycity prediction which was developed in refs. 13, 26, 27 in the framework of the Buran vehicle development till 1988 and which is developing now for the TPM catalycity prediction for entry conditions in the Martian atmosphere [refs. 28-30]. Previously accumulated test experience and current capabilities of the IPG-4 plasmatron from the point of view related to the problem of TPM catalycity are presented. Special attention is paid to the CFD codes as the standard diagnostic tools and to measurements/computations interaction. The previous most important results connected with measured and calculated heat transfer to different test models in high-enthalpy subsonic flows of air, nitrogen, oxygen and carbon dioxide are analyzed. The lessons learned from the development of the combined experimental/numerical methodology, current activities in the field of the thermochemical simulation for re-entry issues and perspectives are discussed.

## 2. Philosophy of the Methodology

The general philosophy of the method for the TPM catalycity prediction on the basis of an induction plasmatron heat transfer experiment developed in refs. 26-30 consists in the tight connection of the catalycity tests with heat transfer simulation for the atmospheric entry conditions. The logic of the surface catalycity determination is based on the stagnation point heat flux measurements in high-enthalpy subsonic flows and the sophisticated techniques of the extraction of the heat flux part, caused by the recombination of atoms, by using the CFD modeling of the heat transfer for test conditions (Fig. 3).

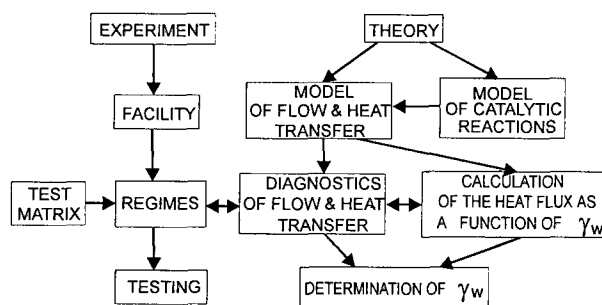


Fig. 3. The logic tree of the methodology for the surface catalycity determination.

This scheme was developed for the study of the catalytic effects in subsonic dissociated air and nitrogen flows in refs. 26, 27, 13 and has been recently applied to the prediction of the catalytic efficiencies of recombination of the  $O$  atoms and  $CO$  molecules on metals, quartz surface, tile coating and antioxidation coating of the carbon-carbon material on the basis of heat transfer experiment carried out in high enthalpy carbon dioxide and oxygen flows [refs. 28-30].

In fact, the method is quite laborious (see the logic scheme on *Fig. 3*), but it reveals a fair way of extrapolation of the surface catalytic effects from ground to flight, at least for the stagnation point heat transfer [refs. 13, 31, 32].

The IPM methodology of the TPM catalycity determination includes the following essential parts:

- 1) production of the highly dissociated subsonic stable gas flows and optimization of the test regimes;
- 2) experimental study of the steady-state heat transfer in the stagnation point configuration;
- 3) tests with different gases;
- 4) precise characterization of the high-enthalpy flows;
- 5) search and application of materials with standard catalytic properties;
- 6) CFD modeling of reacting plasma and gas flows within plasma torch and around a model;
- 7) numerical rebuilding of the free stream enthalpy;
- 8) model of the surface catalycity;
- 9) numerical computations of the nonequilibrium multicomponent boundary layers and design of the heat flux charts for test conditions;
- 10) analysis of uncertainties;
- 11) extrapolation from ground test to the atmospheric entry conditions.

### 3. Facilities

At the middle of the 1970's the plasmatron technology development was turned out from the atmospheric pressure plasmatron IPG-1 [ref. 25] toward low pressure domain due to the Buran program challenges including problem of the TPM catalycity. The development went in directions of the power increasing, the expanding of the pressure range and the enlargement of the discharge channel size. Philosophy of the development at this phase was based on the solution to build two IPG facilities: the first one - oriented on airheating problem coupled with the TPM catalycity, cost-effective samples tests and TPM selection, and the second one - powerful plasmatron for resource tests of the full-scale TPS elements at reentry heating conditions [ref. 17].

The 75-kW IPG-2 plasmatron with the discharge channel 60 mm in diameter produced sub- and supersonic high-enthalpy air and nitrogen flows in the stagnation pressure range 0.05-1 atm and total enthalpy range 10-40 MJ/kg. This facility was used to study of the nonequilibrium heat transfer effects and the TPM catalycity in subsonic dissociated air and nitrogen flows in the pressure range 0.05-1 atm during the period 1978-1988. Few catalycity tests with pure oxygen were performed by the IPG-2. The powerful (1-MW) IPG-3 plasmatron with the

discharge channel of 200 mm in diameter has been operating with air plasma in subsonic regime in the pressure range 0.015-0.1 atm and the same total enthalpy range [ref. 17]. The multipurpose 100-kW IPG-4 plasmatron with the channel of 80 mm in diameter (mass flow rate 1.5-6 g/s) covers the stagnation pressure range 0.01-1 atm in sub- and supersonic regimes with air, nitrogen, oxygen, carbon dioxide and hydrocarbons as working gases.

The inductive plasmatrons IPG-3 and IPG-4 meet requirements [ref. 33] for R&D facilities to simulate reacting flow physics, real surface processes and to carry out code validation. The plasmatron capabilities provide potential possibilities to define well the flow conditions on the basis of judiciously combined surface and flow field measurements and CFD modeling.

### 4. Subsonic Test Regimes

From the standpoint of the TPM catalycity prediction, the subsonic regimes possess three significant advantages over the supersonic ones. Firstly, for hypersonic vehicles with a blunt nose radius  $R_N \sim 1$  m subsonic regimes reveal the way to the duplication of the stagnation point heat transfer if the conditions of a local simulation are satisfied [refs. 13, 31, 32].

Secondly, supersonic plasma flows normally are quite far from equilibrium, whereas the thermodynamic state of subsonic dissociated molecular gas flows in a core is close to LTE at pressures  $\geq 0.1$  atm. Thus, the oxygen flows are completely dissociated in the core, so in fact there is chemical equilibrium in this part of flow. For the carbon dioxide flow at the pressure 0.1 atm the Landau-Teller relaxation time for the CO molecules is  $\tau_{VT} \sim 2 \cdot 10^{-5}$  s, so the relaxation zone length  $\sim 2 \cdot 10^{-3}$  m is much shorter than the distance from the channel exit section to the model ( $6 \cdot 10^{-2}$  m). At the same time the mixing layers and boundary layers near the model should be far from equilibrium.

Finally, in subsonic regimes the boundary layer on a model is quite thick, therefore if the exited molecules are produced on the surface due to the catalytic recombination of atoms those molecules are quenched efficiently within the boundary layer due to collisions [ref. 34]. In this case it is possible to take this effect into account by using the effective rate of catalytic reaction without actual consideration of the process of exited molecules formation.

The choice of the optimal test conditions is very important for reducing flow uncertainties and the contraction of margins. *Fig. 4* taken from ref. 13 shows in the pressure-surface temperature variables the map of the degree of a boundary layer nonequilibrium at the stagnation point of a model with the radius  $R_m = 1.5$  cm flown by a subsonic dissociated nitrogen jet. It is seen, that the conditions within boundary layer can be changed smoothly by pressure variation from frozen boundary

layer toward equilibrium one. The equilibrium region 5 is optimal for calibration, the optimal conditions for catalycity tests could be realized in the region 3 (equilibrium free stream & frozen boundary layer), the influence of the gas-phase reactions on the heat transfer can be studied in the region 4.

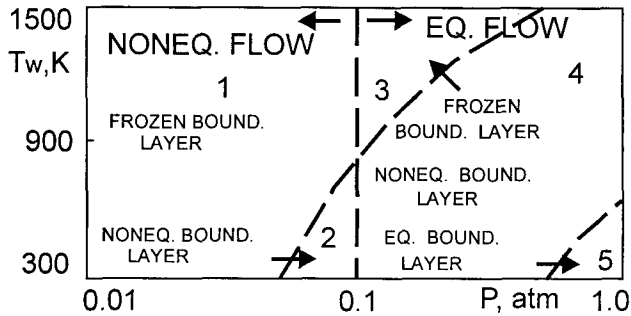


Fig. 4. The map of the degree of a free stream and boundary layer nonequilibrium for subsonic regimes with nitrogen for a model with radius 1.5 cm [ref. 13].

### 5. Test Configuration and Models

In the optimal regimes used, the inductively coupled plasma is forced back from the wall of the quartz tube of the discharge channel by a sublayer of the cold gas, the discharge is stable and exists for a long time. This offers the possibility of studying the heat transfer in the steady-state regimes.

Two main types of the models are used in the heat transfer tests (Fig. 5): 1) the water-cooled copper model with the water flow steady-state heat probes for the stagnation point heat flux measurements; and 2) the model made from SiC material for the TPM testing. The cylindrical models with a flat face of 30-50 mm in diameter are widely used for subsonic tests. During the last 5 years the standard form of the euromodel of 50 mm in diameter with a rounded edge of 11 mm in radius was widely used for high-enthalpy tests [refs. 35, 36, 28-30].

Under typical subsonic test conditions the optimum distance  $Z_m$  between the model and the discharge channel exit can be estimated as  $D_m < Z_m < 2D_c$ , where  $D_m$  is the model diameter and  $D_c$  is the discharge channel diameter. For the IPG-4 tests  $30 \leq Z_m \leq 60$  mm. In the optimum zone the following optimum conditions for the studying of the steady-state heat transfer are realized:

- 1) flow perturbations induced by the model do not reach the discharge channel;
- 2) the flow past the model exposed in the central part of the jet, is close to axisymmetric;
- 3) the high stability of the free jet parameters;
- 4) the uniform heat loading on the sample face;
- 5) the stagnation point heat flux and the surface temperature of the sample are well reproducible;

- 6) the flow enthalpy and velocity along the free-jet axis decrease only slightly.

The variation of the flow parameters and the stationary heat transfer conditions are achieved by the control of the anode power  $N_{ap}$  supplied to the inductor. With the  $N_{ap}$  increasing, the power input in plasma rises, and the flow enthalpy, velocity, stagnation point heat flux and temperature of the sample surface increase respectively.

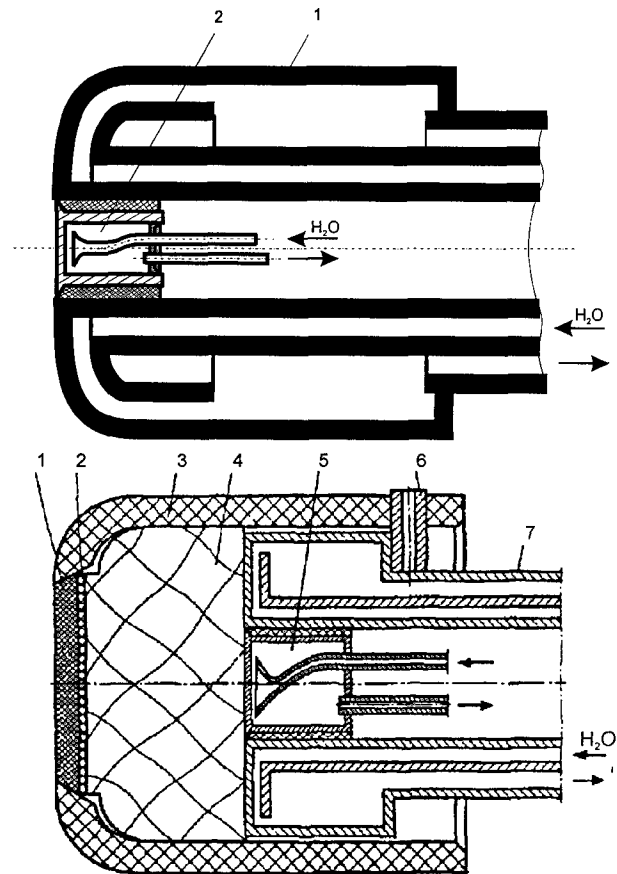


Fig. 5. Models for heat transfer tests in subsonic regimes. upper - model for cooled wall test (refs. 28, 29): 1 - copper body, 2 - water flow stationary heat flux probe; lower - model for catalycity and oxidation tests: 1 - sample, 2 - spacer, 3 - SiC material, 4 - heat insulation, 5 - water flow stationary heat flux probe, 6 - zirconium pin, 7 - water-cooled holder.

### 6. Measurements of the Heat Fluxes to Cooled Surfaces

The water flow steady-state probes made of copper monolith, nickel, monocrystalline molybdenum, quartz of high chemical purity and those made of copper with the heat reception faces covered with silver, platinum, titanium and tantalum were used in cooled wall tests [refs. 26-30]. Those heat-adsorbing surfaces of 14 mm in diameter were polished to a mirror quality. To vary quartz surface temperature at a constant plasmatron operating regime, the quartz probes with the different thickness of the heat reception wall in the range 0.63-2.26 mm are used. In order to improve the reproducibility the probe surface should be cleaned in the plasma flow in the course of a few minutes.

The stagnation point heat flux is calculated by the measured water flow rate through the probe and the water temperature difference between the probe outlet and inlet sections. The water flow rate is measured by the float rotameter with an error of  $\pm 1.5\%$ . The water temperature in the probe is measured by the thermocouples and mercury thermometers with the accuracy of  $0.1^\circ\text{C}$ . The accuracy of the measurement of the stagnation point heat flux to the cooled surface ( $T_w \sim 300\text{ K}$ ) is  $\pm 5\%$ .

For the quartz probes the surface temperature  $T_w$  is obtained by the solution of the 1D heat transfer problem within the heat reception quartz wall taking into account the well documented quartz thermal conductivity [ref. 37]. The well-defined spectral and total quartz surface emissivity for the different wall thickness [refs. 38, 39] are necessary to determine the heat flux  $q_w$ .

The measurements of the heat fluxes to cooled surfaces is one of the key points of the methodology for the TPM catalytic prediction due to two main reasons:

Firstly, cooled wall tests demonstrate the heat effect of the heterogeneous catalysis in dissociated gases [ref. 30]. The difference between the measured values of the heat fluxes to different metals appears as a result of the difference between their surface catalytic activities with respect to atoms recombination. The difference increases with the power input in plasma and, respectively, with the increasing of flow enthalpy, velocity and the degree of dissociation. Since the heat flux to silver wall is higher than that for molybdenum in the dissociated oxygen and carbon dioxide flows, the silver surface is more catalytic than the molybdenum one in those gases.

In the dissociated air and nitrogen the copper and platinum showed the highest catalytic activity but molybdenum also manifested itself as metal with the lowest catalytic [refs. 26, 27] (see Fig. 6).

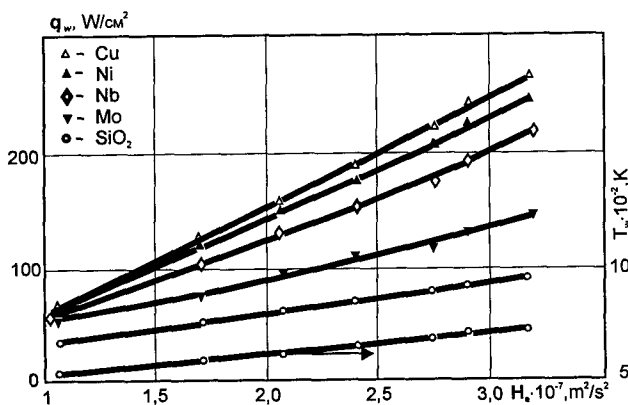


Fig. 6. Catalytic heat effect on cooled metallic surfaces in subsonic dissociated air flows [ref. 26]:  $p=0.1\text{ atm}$ ,  $R_m=1.5\text{ cm}$ .

Secondly, more data for cold surfaces are collected then the experimental heat flux envelope is wider and more information for the validation of the CFD codes can be used. The key point of the methodology is the search of materials with maximum and minimum catalytic efficiencies for the different gas environment. Among the measured heat flux values the maximum one is used for the rebuilding of the flow enthalpy, the minimum one - for the verification of the gas-phase chemistry implemented in the CFD codes for modeling of nonequilibrium flows and heat transfer computations.

### 7. Heat Transfer Measurements for TPM Samples

It should be noted that the convective heat flux to the hot wall can not be measured directly. The stagnation point heat flux to the high temperature surface is rebuilt by the formula:

$$q_w = \varepsilon_{th} \sigma T_w^4 + q_c$$

where  $\varepsilon_{th}$  is the total hemispheric emissivity of the surface,  $\sigma$  is the Stefan-Boltzmann constant,  $T_w$  is the surface temperature,  $q_c$  is the density of the heat loss from the rear sample surface measured by using the water-cooled probe.

The brightness surface temperature of the sample  $T_b$  has to be measured by using optical pyrometers on the basis of the radiation from the heated surface. The operating temperature range should be chosen taking into account the spectral emissivity  $\varepsilon_\lambda$  as a function of the surface temperature. For example, in the temperature measurements for the ceramic tile and quartz surfaces the application of the infrared thermovision system AGA-780 is quite efficient for the brightness temperature record at the wavelength  $5\ \mu\text{m}$  where the spectral emissivity  $\varepsilon_\lambda=0.98$  at  $T_w=300\text{-}1700\text{ K}$  [ref. 38].

The intrinsic surface temperature  $T_w$  is determined taking into account the spectral emissivity  $\varepsilon_\lambda$  of the sample and the spectral transparency  $\tau_\lambda$  of the optical quartz window of the testing chamber by the following formula:

$$T_w = \frac{T_b}{1 + (\lambda T_b / C_2) \ln \varepsilon_{eff}}, \varepsilon_{eff} = \varepsilon_\lambda \tau_\lambda, C_2 = 14380\ \mu\text{K} \cdot \text{K}$$

In the measurements of the surface temperatures of the quartz sample and the ceramic black tile ( $\varepsilon_{th}=0.89\text{-}0.82$  at  $T_w=1200\text{-}1700\text{ K}$ ) by using the POV-80 and APIR-C pyrometers, and the infrared thermovision system AGA-780 the average error is  $\pm 20\text{ K}$  [ref. 28].

In the optical surface temperature measurements the crucial point is the accuracy of the spectral and the total surface emissivity data. The additional uncertainties are connected with the influence of an operational angle of the pyrometric measurements. For the quartz-based borosilicate coating used in the Buran TPS the error in the determination of the heat flux to the surfaces of this kind does not exceed 7%.

## 8. Dynamic Pressure Measurements

The high enthalpy subsonic flow characterization must include the dynamic pressure  $\Delta p$  measurements by using water-cooled Pitot probes at least along the flow axis. In IPM practice the water-cooled Pitot probe made of the same shape as the euromodel for the heat flux measurements (Fig. 5) is used. The dynamic pressure is measured as the difference between stagnation pressure and static pressure at the wall of the test chamber.

The static pressure in the test chamber and the dynamic pressure at the subsonic high-enthalpy flows are measured by using the transducers of "САПФИР" (sapphire) type. The pressure transducer "САПФИР 22М-ДА" model 2030 with the upper limit 125 hPa and the accuracy  $\pm 0.4$  hPa is used for the static pressure measurements. The pressure transducer "САПФИР 22МД-ДД" model 2410 with the upper limit 16 hPa and the accuracy  $\pm 0.02$  hPa is used for the dynamic pressure measurements. The physical principle of the operation is based on the accurate determination of a sensitive sapphire element deformation which is proportional to the measured pressure (or pressure difference). Fig. 7 shows quite specific features of the measured dynamic pressure in subsonic high enthalpy flows [ref. 24]:  $\Delta p$  is a linear function of  $N_{ap}$  and  $\Delta p$  is inversely proportional to  $p$ .

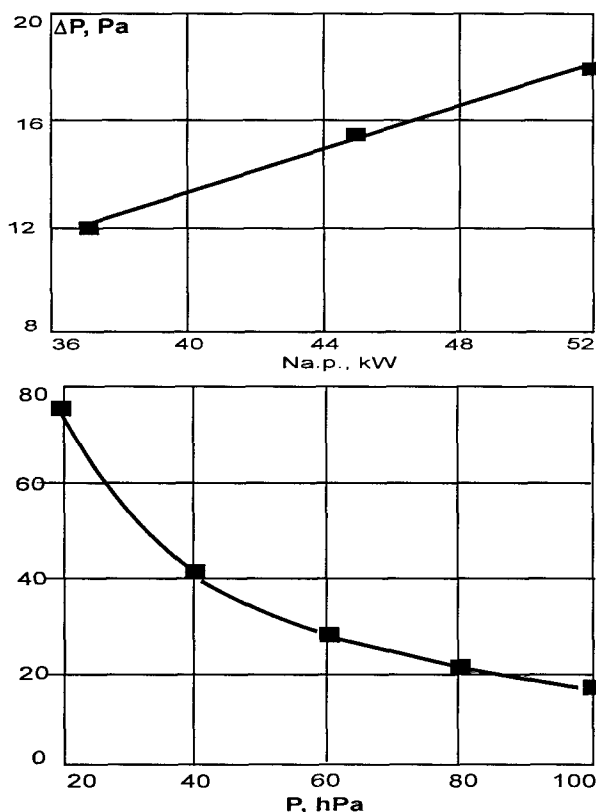


Fig. 7. Dynamic pressure in subsonic carbon dioxide flows as function of the IPG-4 anode power ( $p=100$  hPa) and pressure ( $N_{ap}=45$  kW) at the mass flow rate 1.8 g/s,  $z=60$  mm [ref. 22].

## 9. Logic of the CFD Modeling

At the beginning of the 1980's the general problem of the subsonic high enthalpy test data analysis was the absence of any analytical theory for the stagnation point heat transfer in contrast with super- and hypersonic tests where Fay and Riddell or Gulard's theories [refs. 2, 3] and Newton's solution for a thin shock layer provided sufficient results. So, the application of the full Navier-Stokes equations for the computations of high enthalpy reacting flows for the test conditions at small Reynolds and Mach numbers was the only choice.

The numerical computations of the subsonic plasma and high-enthalpy reacting flows and heat transfer for the plasmatron test conditions is the essential part of the flow characterization and the surface catalycity prediction method [refs. 13, 26, 29, 40]. On the whole, the problem is rather tricky. Up to now the computations of the nonequilibrium molecular plasma flow coupled with the RF electromagnetic field are not in fact. So, our main idea consists in the separation of the whole flow field into three computation zones, where the distinctive flow features can be used for the efficient approach. For the considered plasmatron operating conditions ( $p \geq 0.1$  atm) the main CFD problem for the modeling of the plasma and high-enthalpy oxygen and carbon dioxide reacting flows is divided in the following three problems:

- 1) the equilibrium inductively coupled swirling plasma flow within the cylindrical discharge channel;
- 2) the equilibrium subsonic axisymmetric high-enthalpy laminar jet flow past a cylindrical model;
- 3) the nonequilibrium multicomponent boundary layer with the finite thickness at the stagnation point.

The developed appropriate data base for thermodynamic and transport properties, and soft ware provide efficient numerical modeling for the subsonic regimes of the IPG-4 with different gases (air, nitrogen, oxygen, carbon dioxide, argon).

## 10. Inductive Plasma Modeling

The problem of the inductive plasma flow [ref. 41] is being treated for the case of equilibrium plasmas on the basis of the full Navier-Stokes equations coupled with the simplified Maxwell equations for the RF electromagnetic field [refs. 42, 43]. The statement of the problem includes the plasmadynamics effect of the Lorentz force and the Joule heat release. The 2D Navier-Stokes equations written for the total enthalpy and three velocity components including the tangential component due to the flow swirling and the simplified quasi 1D Maxwell equations for the complex amplitude of the electric field tangential component generating vortical electric currents are used for the computations of reacting plasma flows within the discharge channel. The input parameters of the problem are: the gas composition, the gas flow rate  $\bar{G}$ , the coil geometry, the

electric current frequency  $f$ , and the power input in plasma  $N_{pl}$ .

The boundary conditions at the inlet section and the channel wall should be specified in accordance with the torch design and the system of heat exchange between the torch and the ambient environment. The two main cooling systems are now in use: one self-cooling system with free quartz tube (the IPM plasmatrons, [ref. 17]) and the other with water cooled quartz tube (the VKI plasmatron, [ref. 23]).

In our methodology the finite difference analogies of the Navier-Stokes equations written for the control volumes of the staggered grid are used. The obtained equations are being solved by a method analogous to the SIMPLE method by Patankar and Spalding [ref. 44]. The final system of the linear algebraic equations is being solved by the modified method of incomplete factorization. The simplified equation for the complex amplitude of the electric field is being solved by an effective technique based on the Thomas algorithm.

The transport properties - viscosity, thermal conductivity and electrical conductivity - have to be calculated in advance as the functions of pressure and temperature by the precise formulae of the Chapman-Enskog method in the second approximation by the Sonine polynomials for the plasma viscosity and in the third approximation for the plasma thermal conductivity and electrical conductivity according to well known requirements formulated in ref. 45. The formulation of the plasma transport properties proposed in ref. 46 is very efficient for inductively coupled plasmas computations.

The recent code-to-code validation for the test case with the argon inductively coupled plasma for the IPG-4 plasmatron geometry [ref. 47] has shown rather good agreement between 1D electric field approach [refs. 42, 43] and complete 2D formulation for the plasma induced electric field within the plasmatron channel and in the space beyond the torch itself [ref. 48] for the plasma flow and temperature fields in the whole discharge channel including the plasmatron exit section.

The computed flow and temperature fields for oxygen and carbon dioxide plasmas in the IPG-4 plasmatron discharge channel are shown in Fig. 8 for  $N_{pl}=25$  kW,  $G=2.8$  g/s. The complicated structure of the flow with embedded vortical zones is formed due to the interaction of a swirling gas flow with Joule heat release and magnetic pressure. For both plasmas the flow patterns are quite similar, but the temperature fields are rather different at the same energy input in plasma due to the clear reason: in a carbon dioxide flow the great deal of input energy is spent on dissociation while in fully dissociated oxygen flow an essential part of input energy is pumped in the translational temperature of the monatomic gas.

The calculated flow parameters at the exit section of the discharge channel are the inflow boundary conditions for the second problem of reacting gas flow around a model. Due to the reason mentioned above, in the jet core the velocity and temperature profiles are more smooth for air and carbon dioxide than for oxygen (Fig. 9).

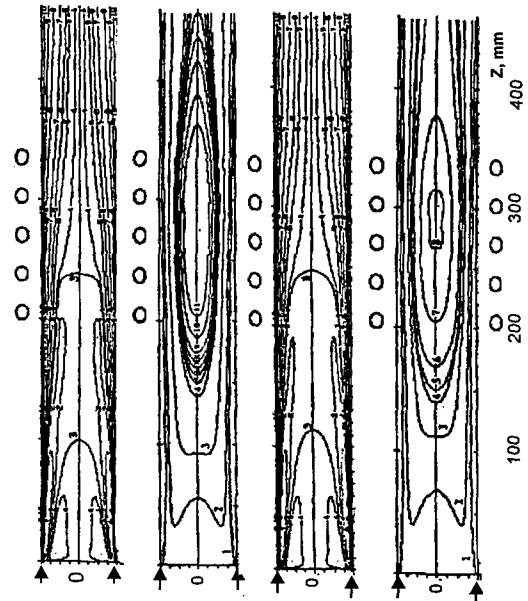


Fig. 8. Flow and temperature fields in the IPG-4 discharge channel for oxygen (left) and carbon dioxide (right) plasmas. Dimensionless stream function values:  $-0.04, -0.02, 0, 0.01, 0.05, 0.1, 0.2, 0.4, 0.6, 0.8$ ; temperature values for the isotherms in 1000 K [ref. 30].

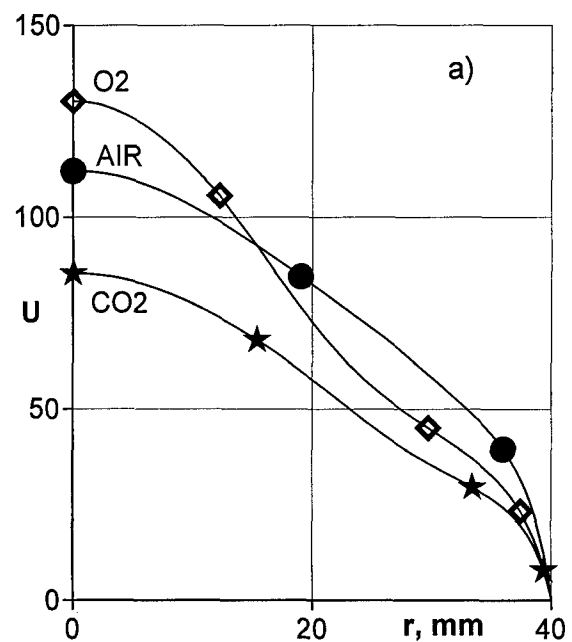


Fig. 9a. Velocity profiles at the exit of the IPG-4 discharge channel for oxygen, air and carbon dioxide plasmas.

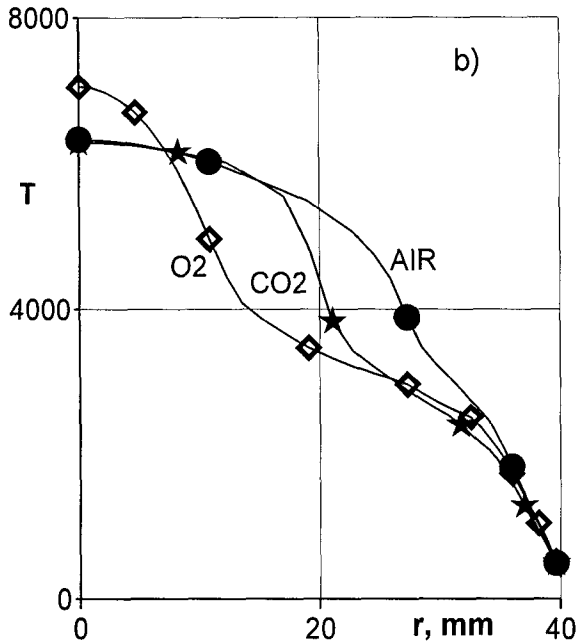


Fig. 9b. Temperature profiles at the exit of the IPG-4 discharge channel for oxygen, air and carbon dioxide plasmas.

### 11. Flow around a Test Model

For the subsonic reacting flow after the plasmatron exit section we can assume that the flow is in equilibrium at pressure  $p \geq 0.1$  atm. In the considered enthalpy range the flow ionization influence on heat transfer is negligible and weak traces of flow vorticity are also not taken into account.

The grounds for the equilibrium approach stand on the specific features of subsonic high-enthalpy flows in plasmatron at pressures  $p \geq 0.1$  atm (see chapter 3 above). The approach consists in the use of equilibrium computations for the incoming subsonic plume serving only as the external solution for the nonequilibrium boundary layer problem. So, the surface catalycity is not an input parameter for this problem.

The full 2D Navier-Stokes equations for the enthalpy, two velocity components and pressure are used for the modeling of the laminar hypersonic ( $M \ll 1$ ) equilibrium high-enthalpy flows over a model (flow swirling is not essential here). It is reasonable to use for computations the same numerical method [ref. 44] which is exploited for the previous problem. Fig. 10 shows the calculated flow and temperature fields of reacting carbon dioxide gas around the model, Fig. 11 - the enthalpy distributions along the jet axis for four different gases. These data confirm (qualitatively) the assumption on the chemical equilibrium in the core of the subsonic jet. In fact, we observe a large isothermal, isobaric zone between the exit section of the discharge channel and the model - favorable conditions for fast relaxation.

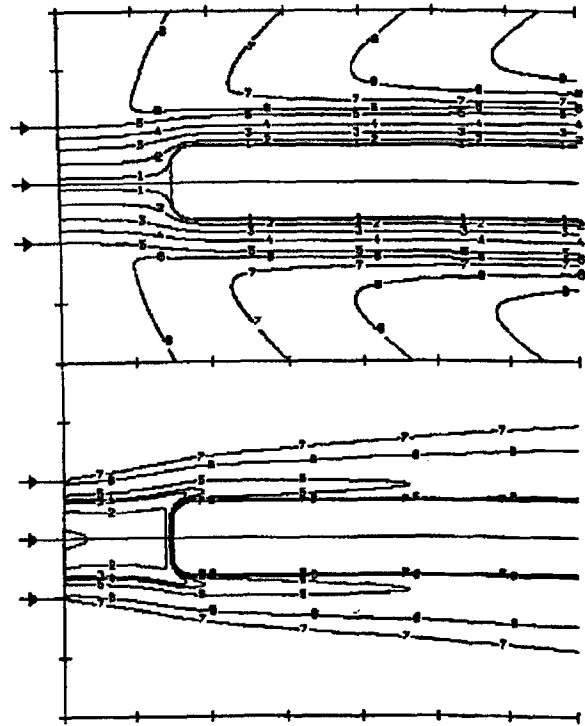


Fig. 10. Flow and temperature fields of reacting carbon dioxide gas flow past a model at  $p=0.1$  atm and  $N_{pl}=25$  kW. Dimensionless stream function values: 0.01, 0.1, 0.3, 0.6, 1.0, 1.2, 1.4, 1.6, 1.8. Temperature values for isotherms: 6500, 6000, 5000, 4000, 2000, 1000 K [ref. 29].

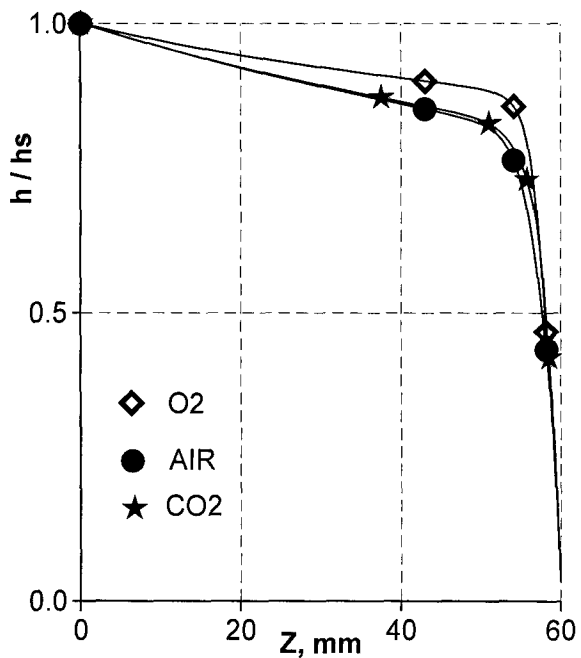


Fig. 11. Dimensionless enthalpy distributions along jet axis from plasmatron exit to a cooled model at  $p=0.1$  atm and  $N_{pl}=20$  kW for different gases.

At low pressures the displacement from equilibrium could be quite essential. The relaxation time  $\tau_{VT} \sim p^{-1}$ , but the hydrodynamic time for inductively coupled plasma has an opposite trend  $\tau_{hyd} \sim p$  and at  $p \sim 0.01$  atm those times are quite comparable.

## 12. Boundary Layer Problem for Subsonic Test Conditions

The analysis of experimental data concerning heat transfer and the procedure of surface catalytic rebuilding require a lot of computations for multiparameter models of the flow and the heat transfer. In spite of the capabilities of the modern PC, the application of the full Navier-Stokes equations, as a standard wind tunnel instrument, for modeling of the nonequilibrium flows in the whole computational field and computations of the heat transfer rates with sufficient accuracy, still does not look effective enough.

In order to find a compromise between requirements to take into account the main features of subsonic viscous reacting jets and heat transfer in plasmatron and to minimize computational efforts, the author developed in the early 1980's the 1D concept of the nonequilibrium boundary layer with finite thickness. This concept made it possible to efficiently separate the problem of the accurate computations of the stagnation point heat transfer rates and the solution of the full Navier-Stokes equations for the flow bulk.

The mathematical model of the 1D flow and heat transfer in the boundary layer for the reacting multicomponent gas presented in refs. 26-30 takes a finite thickness of the boundary layer and flow vorticity at the outer edge of the boundary layer into account by means of the three dimensionless parameters and provides accurate computations of the stagnation point heat flux. These three parameters at the outer edge of the boundary layer have to be obtained from the numerical solution of the full Navier-Stokes equations for the equilibrium subsonic flows around the model. At the fixed value of a gas flow rate those parameters actually slightly depend on the pressure and power input in plasma and should be calculated, as input parameters for the 1D boundary layer code, in advance. After that 1D code can run autonomously in the wide domain of test conditions, surface temperature and catalytic efficiency.

The following assumptions have been made in the physical model of the nonequilibrium boundary layer: 1) gas is a multicomponent mixture of molecules and atoms; 2) molecules vibrations are in equilibrium excitation, chemical kinetics is one-temperature. The data on rate constants for gas-phase reactions have been taken from ref. 49.

The finite difference scheme of the high order of approximation should be used for the fast numerical solution of the 1D boundary layer problem.

## 13. Model of the Surface Catalysis

As we mentioned above, the processes of the formation of molecules due to collisions of atoms on a surface have complex kinetics [ref. 12]. In general, these processes are poorly studied although the kinetics of the oxygen and nitrogen atoms recombination on silica has been investigated in refs. 6, 50, 51. The mechanisms of the Eley-Rideal and Langmuir-Hinshelwood recombination of the oxygen atoms on silica have been studied within a framework of molecular dynamics in ref. 52. Kinetic studies of the catalytic reaction  $CO+O \rightarrow CO_2$  on the quartz-based surfaces, which is important for heat transfer to a vehicle surface during entry into Martian atmosphere, are practically absent.

In our methodology the parameters which characterize surface catalytic have to be determined from the comparison of the measured heat fluxes and surface temperatures with the results of parametric computations (inverse problem). Therefore, the model of surface catalysis has to contain a consistent number of parameters - actually one, or more, if possible to separate contributions of different catalytic reactions in heat transfer by performing tests in different gases.

Here we present the macrokinetic model for the catalytic recombination of the  $O$  atoms and  $CO$  molecules, reactions which accompany the heat transfer from dissociated carbon dioxide to TPM surface, formulated before in ref. 29.

The following assumptions are taken in this rather simple model:

- adsorption of oxygen atoms dominants over other species adsorption;
- adsorption of oxygen atoms and desorption of the products are fast reactions;
- recombination reactions  $O+O \rightarrow O_2$  and  $CO+O \rightarrow CO_2$  follow the Eley-Rideal mechanism  $O+S \rightarrow O_S$ ,  $O+O_S \rightarrow O_2+S$ ,  $CO+O_S \rightarrow CO_2+S$ , where  $S$  is the site,  $O_S$  is the adsorbed oxygen atom (adatom);
- recombination reaction  $C+2O \rightarrow CO_2$  follows the Langmuir-Hinshelwood mechanism  $C+O_S \rightarrow CO_S$ ,  $CO_S+O_S \rightarrow CO_2+S$ .

This scheme leads to the first order reactions of the  $O$  atoms,  $CO$  molecules and  $C$  atoms with three independent effective parameters - catalytic efficiencies  $\gamma_{WO}$ ,  $\gamma_{WCO}$  and  $\gamma_{WC}$  ( $0 \leq \gamma_{Wi} \leq 1$ ). The case  $\gamma_{WO} = \gamma_{WCO} = \gamma_{WC} = 0$  corresponds to a noncatalytic wall, the case  $\gamma_{WO} = \gamma_{WCO} = \gamma_{WC} = 1$  - to a fully catalytic wall.

If  $\gamma_{Wi}$  is identified with effective probability of catalytic recombination of atoms with the number  $i$ , then the boundary conditions for mass fraction of  $i$ -atoms at the wall has the following form

$$-J_i = \rho K_{wi} C_i \quad (13.1)$$

$$K_{wi} = \frac{2\gamma_{wi}}{2 - \gamma_{wi}} \sqrt{\frac{kT_w}{2\pi M_i}} \quad (13.2)$$

Here  $J_i$  is the mass diffusion flux and  $K_{wi}$  is the effective rate of catalytic recombination of  $i$ -atoms (the diffusion velocity of  $i$ -atoms at the wall). If  $\gamma_{wi} \ll 1$ , then

$$K_{wi} = \gamma_{wi} \sqrt{\frac{kT_w}{2\pi M_i}} \quad (13.3)$$

In literature the last expression occurs more frequently, then the exact expression.(13.2). For a low catalytic wall it is quite accurate, practically if  $\gamma_{wi} \leq 0.1$ . But in the full range of  $\gamma_{wi}$  the formula (13.3) is incorrect, because it was obtained for the case when the distribution function of atoms was assumed to be Maxwell function. If the wall is sufficiently catalytic, it disturbs the Maxwell distribution due to the gradient of atomic fraction and diffusion velocity becomes different from the thermal velocity of atoms.

In addition to the boundary conditions (13.1) the conditions of the total mass balance and mass balance of atoms at the surface must be added. For example, for 5-species dissociated carbon dioxide mixture ( $CO_2$ ,  $CO$ ,  $O_2$ ,  $O$ ,  $C$ ) the following necessary conditions of the  $O$  and  $C$  atoms balance must be implemented in the 1D boundary layer code:

$$J_{O_2} + \frac{2M_O}{M_{CO_2}} J_{CO_2} + \frac{M_O}{M_{CO}} J_{CO} + J_O = 0,$$

$$\frac{M_C}{M_{CO_2}} J_{CO_2} + \frac{M_C}{M_{CO}} J_{CO} + J_C = 0$$

#### 14. Numerical Rebuilding of Flow Parameters

The characterization of the free stream conditions (velocity, pressure, enthalpy, chemical composition) is the crucial point in the problem of the TPM catalytic prediction from the heat transfer test. The diagnostic of high-enthalpy reacting gas flows still is a quite challenging problem. In fact, we have to predict reliable data on the TPM catalytic on the basis of incomplete information on a plasma flow in facility.

It is essential to understand that the quality of the result is quite sensitive to the choice of the test regimes. For subsonic tests the main flow uncertainties are connected with the jet nonuniformity and displacement from equilibrium. So, it is vital to find optimal test regimes and then to determine profiles of the parameters (not only local or average values).

For the subsonic test conditions located in the optimal region (see Fig. 4) it is necessary to measure at least two flow parameters - the enthalpy and head velocity. The direct enthalpy measurements still are not in fact because there are not standard conditions for calibration, and any theory of an enthalpymeter with an accurate analysis of coupled effects of a nonequilibrium boundary layer does not exist.

The experimental key point of our methodology is a measurement of the stagnation point heat flux to the cooled surface with a standard high catalytic efficiency. The search of surfaces with such extreme property is an indispensable step for TPM catalytic prediction. After a considerable number of plasma tests performed with different metals it was found that in dissociated air and nitrogen flows the copper and platinum are the best catalysts [refs. 26, 27, 17], in dissociated oxygen and carbon dioxide flows the silver has the same feature [refs. 29, 30]. So, the measurements of heat transfer to the cooled wall is one of the stepping stones to TPM catalytic prediction.

The next one - the steady state measurements of the dynamic pressure of the high-enthalpy subsonic flow which were discussed in the chapter 8. Those two measured parameters are necessary and sufficient for the rebuilding of flow conditions if the flow core is in equilibrium, the measured maximum heat flux is related to a fully catalytic wall and hydrodynamic parameters are derived from the CFD modeling. In this case the free stream velocity and thermodynamic parameters at the flow axis can be determined from the numerical solution of the following nonlinear algebraic equations:

$$q_w = 0.763 Pr^{-0.6} (\rho_e \mu_e)^{1/2} \left(\frac{V_S}{R_{eff}}\right)^{1/2} \left(\frac{\rho_w \mu_w}{\rho_e \mu_e}\right)^{0.1} (h_e - h_w)$$

$$\Delta p = k(Re) \rho_e V_S^2 / 2, \quad p = \rho_e R T_e / m_e, \quad F(p, T_e, c_{ie}) = 0$$

Here, the first formula is the Fay-Riddell formula [ref. 2] adapted and verified for subsonic flows, the last formulae are the chemical equilibrium equations for the considered gas mixture,  $q_w$ ,  $\Delta p$  are the measured parameters,  $k(Re)$  is the coefficient which takes into account the effect of the viscosity at low Reynolds numbers  $Re$ ,  $R_{eff}$  is the effective radius of the model which depends on the flow geometry, the model and channel radii  $R_m$  and  $R_c$ .

The geometrical parameter  $R_{eff}$  is expressed in term of the velocity gradient at the model stagnation point  $R_{eff} = V_S (dU_e/dr)_0^{-1}$  and must be determined from the numerical solution of the Navier-Stokes equations for the subsonic flow past a model.

For the IPG-4 plasmatron with the discharge channel of 80 mm in diameter and the standard euromodel with a flat face and 50 mm in diameter at the stagnation point

configuration  $R_{eff} = 1.28 R_m$ . The formulae of kinetic theory for transport properties should be included in the procedure described above.

The results of this procedure application for the rebuilding of the subsonic high enthalpy carbon dioxide flow conditions as the functions of the generator anode power at the pressure 0.1 atm are presented in Fig. 12.

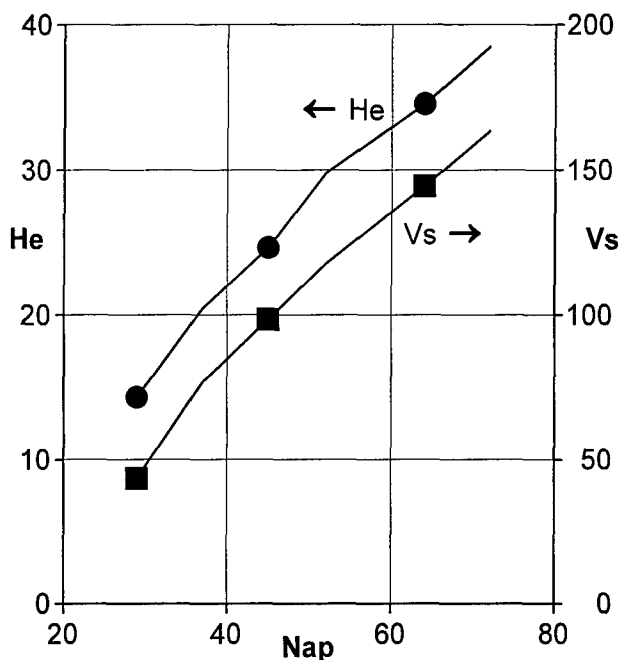


Fig. 12. Enthalpy (MJ/kg) and velocity (m/s) of carbon dioxide flow at the center of the plasmatron exit as functions of anode power at  $p=0.1$  atm and  $G=1.8$  g/s.

### 15. Procedure of the TPM Catalytic Determination

Let's consider the catalytic determination technique for the case when the surface is being flown by high enthalpy gas which is a binary mixture of atoms and molecules (dissociated nitrogen or oxygen). The first step consists in the study of the heat transfer to a cold wall from both sides - experimental and numerical. In the experimental part it is important to perform tests with different cooled metallic surfaces - as many as possible - and to put the data in the order of catalytic efficiency. At this step the traditional presentation of the calculated heat fluxes as the functions of  $\gamma_w$  in S-like curves is required (see Fig. 13 with data for tests in high enthalpy nitrogen flows in the IPG-2 plasmatron).

The search of the standard material with the minimal catalytic efficiency is also a key point. The heat flux from a nonequilibrium boundary to a noncatalytic wall ( $\gamma_w=0$ ) is quite sensitive to gas-phase recombination of atoms. So, the comparison of numerical data for this case with the measured minimal heat flux reveals the way to verify the data on the rates of the atom-atom recombination implemented in the CFD codes. If an experimental point drops out of the numerically predicted heat flux range, bounded below with the

minimum corresponding to  $\gamma_w=0$ , that means that the rate of atom-atom recombination is the excessive one. In this way we found [refs. 27, 30] that the data for nitrogen and oxygen atom-atom recombination from ref. 53 had provided the excessive rates. So, standard noncatalytic materials are indispensable tools for the validation of data base for the gas-phase chemistry.

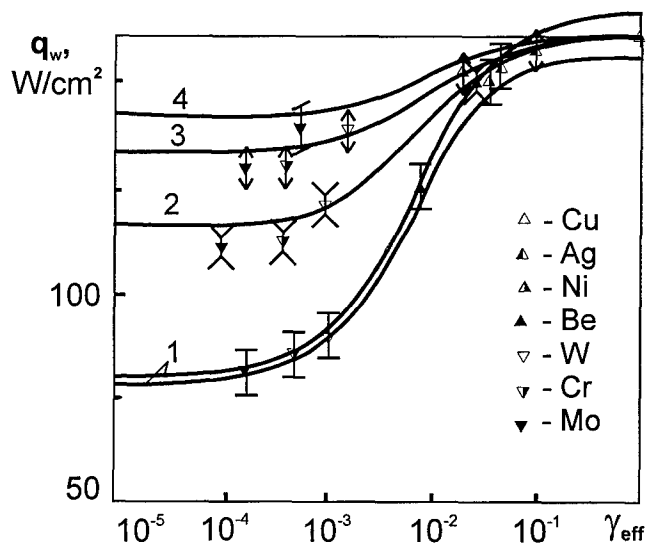


Fig. 13. Stagnation point heat fluxes to cooled surfaces in dissociated nitrogen flows as functions of catalytic efficiency at different pressures [ref. 26]. Dots - measurements, curves - calculations: 1 - 0.1 atm, 2 - 0.2 atm, 3 - 0.3 atm, 4 - 0.4 atm. IPG-2,  $h_e=21$  MJ/kg,  $R_m=1.5$  cm.

The CFD modeling produces a lot of information and a quite important question about the presentation of numerical data in the way mostly convenient for the experimental data analysis turns up. Concerning the TPM catalytic prediction, the method of a heat transfer chart, proposed by the author at the beginning of 1980's, still remains very efficient. A whole spectrum of the heat transfer conditions can be presented by the one heat flux chart in  $q_w-T_w$  coordinates (measured parameters) for the given test regime and model geometry.

As an example, Fig. 14 presents the heat flux chart for the subsonic test with pure nitrogen performed by the IPG-2 plasmatron at the pressure 0.1 atm, enthalpy  $h_e=20$  MJ/kg and for a cylindrical model with a flat face of 30 mm in diameter. The solid curves are the dependencies  $q_w(T_w)$  at constant  $K_w$  values ( $0 \leq K_w \leq \infty$ ). The upper curve 1 corresponds to a fully catalytic surface ( $K_w=\infty$ ), the lower curve - to a noncatalytic surface ( $K_w=0$ ). The dash curve presents the heat transfer rate to the noncatalytic surface calculated for the frozen boundary layer, i.e. the lower theoretical limit for the heat flux. The actual calculated heat flux envelope is bounded from the right side by the curve  $q_w=\epsilon_{th}\sigma T_w^4$ , which corresponds to radiative-equilibrium wall, so, the right border is depended from the TPM optical properties.

The location of an experimental point is determined by two measured coordinates  $q_w$  and  $T_w$ . The measured heat fluxes to the cooled copper surface ( $T_w=300$  K) were used as a caliber value of the heat flux to the fully catalytic wall. So, the upper left corner of the chart in Fig. 14 is matched with the experimental point, presented the copper cooled surface. Each experimental point gives one value of surface catalycity (for one measured temperature value), which is determined by the point position relative to curves  $\gamma_w = \text{const}$ .

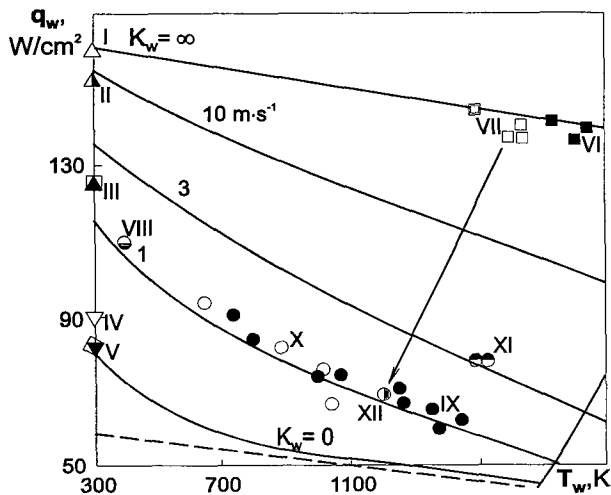


Fig. 14. Heat flux chart and experimental data for the subsonic test with pure nitrogen [ref. 17]. IPG-2:  $p=0.1$  atm,  $h_e=20$  MJ/kg,  $V_s=160$  m/s,  $R_m=1.5$  cm. I - Cu, II - Ni, III - Be, IV - W, V - Mo, VI - pyrographite, VII - carbon, VIII -  $\text{SiO}_2$  coating, IX - ceramic tile, X - quartz, XI - C-C with antioxidation coating, XII -  $\text{SiO}_2$  coating on carbon; dash line - frozen boundary layer with  $K_w=0$ .

All data for cold metals are located along the left border of the heat flux envelope in the Fig. 14. The minimum of the measured heat flux corresponds to molybdenum. The data for quartz and tile coating are gathered along the curve which corresponds to  $K_w \approx 1 \text{ m/s}$  ( $\gamma_w \approx 3 \cdot 10^{-3}$ ), which means that the catalytic efficiency of the quartz-based surfaces does not depend sufficiently on surface temperature in the case of atomic nitrogen recombination.

The heat flux chart for the subsonic test with pure oxygen performed recently by using the IPG-4 plasmatron at the pressure 0.1 atm, for the euromodel configuration looks quite similar (Fig. 15). We can find from Fig. 14 and 15 that the catalytic efficiencies of the quartz-based materials in dissociated nitrogen and oxygen flows are rather close.

For a multicomponent mixture the several catalytic efficiencies should be determined from catalycity tests: at least two for 5-species dissociated air and carbon dioxide to characterize the catalytic reactions  $\text{O}+\text{O} \rightarrow \text{O}_2$  ( $\gamma_{\text{WO}}$ ),

$\text{N}+\text{N} \rightarrow \text{N}_2$  ( $\gamma_{\text{WN}}$ ) in air and  $\text{O}+\text{O} \rightarrow \text{O}_2$  ( $\gamma_{\text{WO}}$ ),  $\text{CO}+\text{O} \rightarrow \text{CO}_2$  ( $\gamma_{\text{WCO}}$ ) in carbon dioxide. In fact, it is possible to rebuilt only one parameter of the surface catalycity using the present methodology.

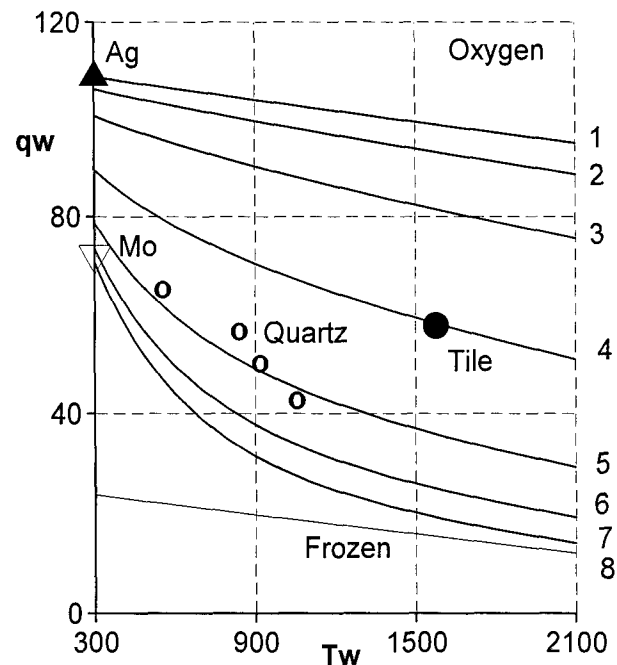


Fig. 15. Heat flux chart and experimental data for the subsonic test with pure oxygen [ref. 30]. IPG-4:  $p=0.1$  atm,  $h_e=20$  MJ/kg, euromodel with  $R_m=2.5$  cm; curves 1-7:  $\gamma_w=1, 10^{-1}, 3 \cdot 10^{-2}, 10^{-2}, 3 \cdot 10^{-3}, 10^{-3}, 0$ .

Therefore, for those mixtures one parameter must be specified in advance on the basis of tests performed in simple gases, or we have to introduce some average catalytic efficiency for the two or more reactions. We see from the data presented in Fig. 14 and 15 that we can use such effective catalycity assuming that  $\gamma_{\text{WO}} = \gamma_{\text{WN}}$  for the quartz-based materials in dissociated air.

The one calculated chart of the stagnation point heat flux is shown on Fig. 16 for the subsonic test with carbon dioxide performed by the IPG-4 plasmatron at  $p=0.1$  atm,  $N_{ap}=45$  kW ( $h_e=21.2$  MJ/kg). The equality  $\gamma_{\text{WCO}} = \gamma_{\text{WO}} = \gamma_w$  was assumed in the surface catalycity model. The upper solid curve 1 corresponds to a complete  $\text{CO}_2$  reduction ( $\gamma_w=1$ ), the lower curve 7 - to a noncatalytic surface ( $\gamma_w=0$ ). All experimental data for quartz are spaced along the curve 5 ( $\gamma_w=3 \cdot 10^{-3}$ ). Those data and the data shown in Fig. 15 justify the above mentioned assumption  $\gamma_{\text{WCO}} = \gamma_{\text{WO}}$  for the quartz-based materials.

But in general, one should be careful when an average catalytic efficiency is being introduced. For example, it is incorrect for the surface catalycity on a cold titanium surface in dissociated air. As was found in ref. 26, the catalytic recombination of the O and N atoms on titanium have quite different efficiencies:  $\gamma_{\text{WN}}=0$ ,  $\gamma_{\text{WO}}=10^{-2}$ . Due to this difference the effect of the anomalous increasing of

heat transfer to the titanium surface exposed in dissociated nitrogen flow was observed when oxygen was slightly injected from surface into the boundary layer (Fig. 17, [ref. 54]).

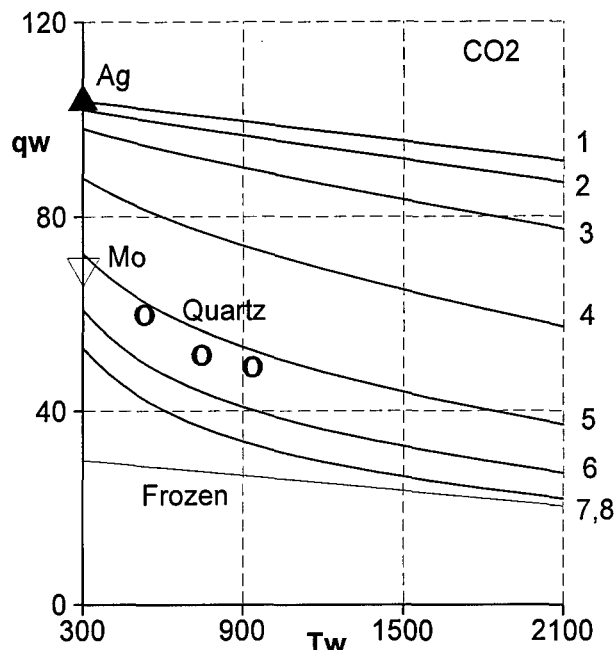


Fig. 16. Heat flux chart and experimental data for the subsonic test with carbon dioxide [refs. 29, 30]. IPG-4:  $p=0.1$  atm,  $h_e=30$  MJ/kg, euromodel with  $R_m=2.5$  cm; curves 1-7:  $\gamma_w=1, 10^{-1}, 3 \cdot 10^{-2}, 10^{-2}, 3 \cdot 10^{-3}, 10^{-3}, 0$ .

This effect was caused by the formation of oxygen atoms near the surface and their diffusion toward surface which was quite catalytic to O atoms recombination. Therefore, heat flux was increasing in comparison with heat flux to noncatalytic wall (in pure nitrogen).

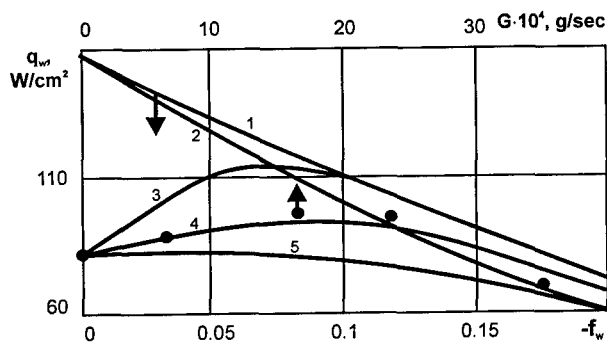


Fig. 17. Effect of the stagnation point heat flux increasing at a weak injection of the oxygen into nonequilibrium boundary layer near the titanium surface exposed in flow of the dissociated nitrogen [ref. 50];  $G$  - mass flow rate of oxygen,  $f_w$  - dimensionless stream function; 1 -  $K_{WO}=K_{WN}=10^4$  m/s; 2 -  $K_{WO}=0, K_{WN}=10^4$  m/s; 3 -  $K_{WO}=10^4$  m/s,  $K_{WN}=0$ ; 4 -  $K_{WO}=2$  m/s,  $K_{WN}=0$ ; 5 -  $K_{WO}=K_{WN}=0$ .

## 16. Discussion

On the basis of the presented self-consistent experimental-theoretical methodology the efficiencies of the catalytic recombination of the N and O atoms, and CO molecules were extracted from high enthalpy tests with dissociated nitrogen, air, oxygen and carbon dioxide flows performed by using the IPG-2 and IPG-4 plasmatrons in subsonic regimes at pressure  $p \geq 0.1$  atm, when free streams in the cores were close to the thermal and chemical equilibrium. The appropriate CFD codes and methodology for the modeling of the whole flow field in the plasmatrons and the rebuilding of the free stream conditions were developed.

Normally, one test regime gives one value of  $\gamma_w$  for the appropriate surface temperature. In order to obtain the dependence  $\gamma_w(T_w)$  the variation of the free stream parameters, the different test models and heat probes were used in experiment. A lot of computations were carried out in order to analyze the test data. As an example, Fig. 18 presents in the Arrhenius coordinates data for  $\gamma_{WO}$  and average efficiency  $\gamma_w$  obtained in pure oxygen and carbon dioxide subsonic gas flows for quartz and tile coating [refs. 28-30]. Taking into account some scattering of the data we can see that the presented data are in satisfactory agreement with the well known data on the recombination of oxygen atoms on quartz from ref. 55 and on RCG presented in ref. 5.

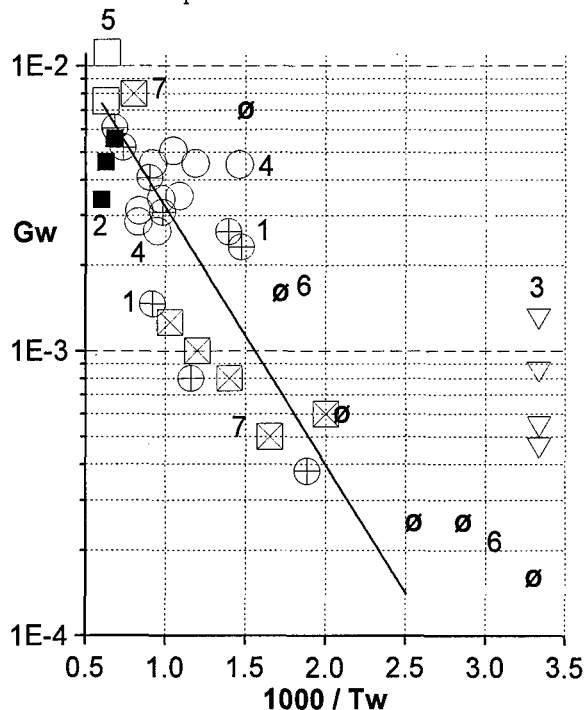


Fig. 18. Surface catalytic efficiency versus temperature in carbon dioxide and oxygen [refs. 28-30]. Carbon dioxide: 1 - quartz, 2 - tile, 3 - molybdenum; Oxygen: 4 - quartz, 5 - tile, 6 - quartz (ref. [55]), 7 - RCG (ref. [5]).

The data on the quartz average catalytic efficiency in carbon dioxide flows have a slight temperature dependency and almost Arrhenius like behavior. On the

whole, the data for  $\gamma_{WO}$  are quite close to the data for the average efficiency  $\gamma_W$  obtained from tests with carbon dioxide. A good agreement between the efficiency of the catalytic reaction  $O+O\rightarrow O_2$  and the average efficiency of the catalytic reactions  $O+O\rightarrow O_2$ ,  $CO+O\rightarrow CO_2$  on a quartz surface confirms the simple model of catalysis proposed in ref. 29.

It appeared that catalytic efficiencies of the Buran tile coating in dissociated air and carbon dioxide flows are quite close. Our recent data on atomic oxygen and carbon monoxide catalytic recombination [refs. 29, 30] have shown the maximum in the dependence  $\gamma_W(T_W)$  at  $T_W\approx 1670$  K and the decreasing  $\gamma_W$  at higher temperatures due to the high efficiency of the atomic oxygen surface desorption. The numerical analysis of the experimental data obtained from tests with dissociated air, carbon dioxide and pure oxygen flows has revealed the similarity between the heterogeneous recombination mechanisms on the ceramic tile surface in the dissociated air and carbon dioxide gas flows and pointed out the atomic oxygen adsorption-desorption and recombination as dominant factors in catalytic processes accompanying the vehicles entry in the Earth and the Martian atmospheres.

### Conclusion & Outlook

The inductive plasmotrons of the IPG family appeared as necessary and capable ground tools for the simulation of the real gas phenomena and plasma/surface interaction during the Buran vehicle campaign in 1978-1988. The catalytic efficiencies of the black ceramic tile surface and antioxidation coating of the C-C material theoretically predicted from the IPG-2 and IPG-4 plasmotrons tests were completely confirmed in flight experiments with the Bor and Buran vehicles. Recent researches [refs. 24, 28-30, 32] have revealed good capabilities of the IPG-4 plasmatron for the simulation of thermochemical loads on heat shields of the Mars Pathfinder and future Mars Probe vehicles [ref. 56], including surface catalysis effects.

One of the main lessons learned from the previous experience in inductive plasma applications in the atmospheric reentry problem - the necessity of the CFD codes implementation as standard tools for the characterization of the high-enthalpy facilities and for the prediction of the surface catalycity. Another lesson: CFD models must be verified in the whole possible operating domain. Any disagreement between the measured and computed data should be accepted as a positive motivation for the validation of both parts of the collected information on flow conditions and heat transfer parameters.

Apparently inductive plasmotrons have powerful potential capabilities for future challenges. The nearest problems are connected with uncertainties of nonequilibrium inductively coupled plasma flows and

TPM catalycity prediction at low pressures  $\sim 10^{-2}$  atm. Judicious CFD codes for multi-temperature sub- and supersonic reacting plasma flows computations must be developed and combined with precise measurements of the enthalpy and flow fields including the emission spectroscopy analysis within the flow core and boundary layers. Precise techniques for the characterization of the TPM optical properties at high temperatures should be included into the list of standard plasmatron measurements. For the promising inductive plasma applications to sample return missions the operating envelope has to be expanded toward the pressures above 1 atm. In this field the coupled problem of the RF discharge plasmadynamics and radiative gasdynamics is coming fast.

### Acknowledgements

The preparation of this paper was supported by RTA contract 4329A and the work performed in part under the ISTC project 036. The author would like to express his gratitude to Prof. J.F. Wendt, Prof. M. Carbonaro and Prof. J.-M. Charbonnier for inviting to the VKI at the RTA/AVT Special Course, and to thank Dr. S. Vasil'evskii, V. Mysova and N. Mamyrkina and for help in figures design.

### References

1. Bonhoeffer, K. F., *Zeits. f. Physik. Chemie.* 1924, v. 113, No. 3, p. 199.
2. Fay, J. A. and Riddell, F. R., "Theory of Stagnation Point Heat Transfer in Dissociated Air," *J. Aeronaut. Sci.*, 1958, v. 25, No. 2, p. 73.
3. Goulard, R., "On Catalytic Recombination Rates in Hypersonic Stagnation Heat Transfer," *Jet Propulsion*, 1958, v. 28, No. 11, p. 737.
4. Scott, C. D., "Catalytic Recombination of Nitrogen and Oxygen on High Temperature Reusable Insulation," *Progress in Astronautics and Aeronautics*, 1981, v. 77, ed. by A. L. Crosbie, AIAA, New York, p. 192.
5. Stewart, D. A., Rakich, J. V., and Lanfranco, M. J., "Catalytic Surface Effects Experiment on the Space Shuttle," *Progress in Astronautics and Aeronautics*, 1982, v. 82, ed. by T. E. Horton, AIAA, New York, p. 248.
6. Jumper, E. J., "Recombination of Oxygen and Nitrogen on Silica-Based Thermal Protection Surfaces: Mechanism and Implications," in: *Molecular Physics and Hypersonic Flows*, 1996, NATO ASI Series, v. 482, ed. by M. Capitelli, Kluwer, p.203.
7. Lozino-Lozinskii, G. E., "Buran Flight," in: *Gagarin Scientific Studies in Aviation and Cosmonautics*, 1989 (in Russian), Nauka, Moscow, 1990, p. 6.
8. Voinov, L.P., Zalugin, G.N., Lunev, V.V., and Timoshenko, V.P., "Comparative Analysis of Laboratory and Full-Scale Data Concerning "Bor"

- and "Buran" Space Vehicles Thermal Protection Material Catalycity," *Cosmonautics and Rocket Engineering* (in Russian), TSNIIMASH, 1994, No. 2, p. 51.
9. Baronets, P.N., Kolesnikov, A.F., Kubarev, S.N., Pershin, I.S., Trukhanov, A.S., Yakushin, M.I., "Overequilibrium Heating of the Surface of a Heat-Shield Tile in a Subsonic Jet of Dissociated Air," *Fluid Dynamics*, Plenum, (tr. from Russian), 1991, v. 26, No. 3, p.437.
  10. Gupta, R.N., Lee, K.P., Scott, C.D., "Aerothermal Study of Mars Pathfinder Aeroshell," *J. of Spacecraft and Rockets*, 1996, v. 33, No.1, p. 61.
  11. Gromov V.G., Afonina N.E., "Thermochemical Nonequilibrium Computations for a Mars Probe," 3rd European Symposium on Aerothermodynamics for Space Vehicles, ESTEC, Noordwijk, The Netherlands, 24-26 November 1998, ESA SP-426, 1999, p. 179.
  12. Hardy W.A., Linnett J.W., "Mechanism of Atom Recombination on Surface," *Proc. of 11-th Int. Symp. on Combustion*. Berkley, Ca., 1966, p.167.
  13. Kolesnikov, A.F., "The Aerothermodynamic Simulation in Sub- and Supersonic High- Enthalpy Jets: Experiment and Theory," *Proc. of the Second European Symposium on Aerothermodynamics for Space Vehicles*, ESTEC, Noordwijk, The Netherlands, November 1994, ESA SP-367, 1995, p. 583.
  14. Babat, G.I., "Electrodeless Discharges and Some Allied Problems," *J. of Inst. of Electr. Engineers*, III, 94, issue 27, 1947, p.27.
  15. Reed, T.B., "Induction-coupled Plasma Torch," *J. of Appl. Phys.*, v. 32, 1961, p.821.
  16. Yakushin, M.I., "Production of the High Temperature Gas in Electrodeless Induction Discharge," *Prikl. Mech. Tech. Phys.* (in Russian), No. 3, 1969, p.143.
  17. Gordeev, A.N., Kolesnikov, A.F., Yakushin, M.I., "An Induction Plasmatron Application to 'Buran's' Heat Protection Tiles Ground Tests," *SAMPE Journal*, v. 28, No. 3, 1992, p. 29.
  18. Anfimov, N.A., "TsNIIMASH Capabilities for Aerogasdynamical and Thermal Testing of Hypersonic Vehicles," *AIAA 92-3962*, 1992.
  19. Labaste, V., Kolesnikov, A., Ferenbach, L., Guegan, H., Guigue-Joguet, P., "Influence of Aging upon Catalycity of C/C Material Protected Against Oxydation", *Proc. of the Intern. Symposium on Advanced Materials for Lightweight Structures '94*. ESTEC, Noordwijk, The Netherlands, 22-25 March 1994, p. 273.
  20. Auweter-Kurtz, M., Kurtz, H.L., Laure, S., "Plasma Generators for Re-Entry Simulation", *J. Propulsion and Power*, v. 12, No.6, November 1996, p. 1053.
  21. Auweter-Kurtz, M., Hammer, F., Herdrich, G., Kurtz, H., Laux, T., Schreiber, E., Wegmann, T., "The Ground Test Facilities for TPS at The Institut Fur Raumfahrtsysteme", 3rd European Symp. on Aerothermodynamics for Space Vehicles, ESTEC, Noordwijk, The Netherlands, November 24-26, 1998, ESA SP-426, 1999, p. 529.
  22. Bascele, J.M., Conte, D., Leroux, R., "A New Test Facility for Experimental Characterization of High Temperature Composites and Ceramics", 3rd European Workshop on TPS. ESTEC, Noordwijk, The Netherlands, 25-27 March 1998.
  23. Bottin, B., Carbonaro, M., Paris, S., Van Der Haegen, Novelli, A., Vennemann, D., "The VKI 1.2 MW Plasmatron Facility for the Thermal Testing of TPS Materials", 3rd European Workshop on TPS. ESTEC, Noordwijk, The Netherlands, 25-27 March 1998. Netherlands, 25-27 March 1998.
  24. Bykova, N. G., Vasil'evskii, S. A., Gordeev, A. N., Kolesnikov, A. F., Pershin, I. S., and Yakushin, M. I., "An Induction Plasmatron Application for Simulation of Entry into Martian Atmosphere," 3rd Int. Symp. on Environmental Testing for Space Programmes, ESTEC, Noordwijk, The Netherlands, 24-27 June 1997, SP-408, 1997, p. 195.
  25. Georg, E.B., Yakushin, M.I., "Thermal Boundary Layer on Models Disintegrating in a High-Enthalpy Gas Stream," *Fluid Dynamics*, Plenum, (tr. from Russian), v. 11, No. 1, 1976, p. 21.
  26. Kolesnikov, A.F. and Yakushin, M.I., "Determination of Heterogeneous Recombination Effective Probabilities of Atoms from Heat Fluxes to the Surface in Dissociated Air Flow," *Matematicheskoe Modelirovanie* (in Russian), 1989, v. 1, No. 3, p.44.
  27. Vasil'evskii, S.A., Kolesnikov, A.F., and Yakushin, M.I., "Determination of the Effective Probabilities of the Heterogeneous Recombination of Atoms When Heat Flow is Influenced by Gas-Phase Reactions," *High Temperature*, Plenum, (tr. from Russian), 1991, v. 29, No. 3, p. 411.
  28. Bykova, N.G., Vasil'evskii, S.A., Gordeev, A.N., Kolesnikov, A.F., Pershin, I.S., and Yakushin, M.I., "Determination of the Effective Probabilities of Catalytic Reactions on the Surfaces of Heat Shield Materials in Dissociated Carbon Dioxide Flows", *Fluid Dynamics*, Plenum, (tr. from Russian), 1997, v.32, No. 6, p. 876.
  29. Kolesnikov, A.F., Pershin, I.S., Vasil'evskii, S.A., and Yakushin, M.I., "Study of Quartz Surface Catalycity in Dissociated Carbon Dioxide Subsonic Flows," 1998, *AIAA 98-2847*.
  30. Kolesnikov, A., Yakushin, M., Vasil'evskii, S., Pershin, I., and Gordeev, A. "Catalysis Effects on Quartz Surface in High-Enthalpy Oxygen & Carbon Dioxide Flows", 3rd European Symposium on Aerothermodynamics for Space Vehicles, ESTEC, Noordwijk, The Netherlands, 24-26 November 1998, ESA SP-426, 1999, p. 537.
  31. Kolesnikov, A.F., "Conditions of Simulation of Stagnation Point Heat Transfer from a High-Enthalpy

- Flow," Fluid Dynamics, Plenum, (tr. from Russian), 1993, v. 28, No. 1, p. 131.
32. Kolesnikov, A., "The Concept of The Local Thermo-Chemical Simulation for Re-Entry Problem: Validation & Applications", presented in 9th Thermal & Fluids Analysis Workshop, August 31 - September 4, 1998, NASA Lewis Research Center and Ohio Aerospace Institute, Cleveland, Ohio.
  33. Wendt, J.F., Muylaert, J.M., "Status of Hypersonic Testing Capabilities in Europe", Proc. of the Second European Symposium on Aerothermodynamics for Space Vehicles, ESTEC, Noordwijk, The Netherlands, November 1994, ESA SP-367, 1995, p. 165.
  34. Berkut V.D., Doroshenko V.M., Kovtun V.V., and Kudryavtsev N.N. Nonequilibrium Physico-Chemical Processes in Hypersonic Aerodynamics. Moscow, Energoatomizdat (in Russian). 1994, 400p.
  35. Gulhan, A., Vennemann, D., Yakushin, M., and Zhestkov, B., "Comparative Oxidation Tests on Reference Material in Two Induction Heated Facilities," 46th Int. Astronautical Congress, October 2-6, 1995, Oslo, Norway.
  36. Vennemann, D., and Yakushin, M., "Oxidation Tests on SiC Reference Material in an Induction Heated Facility under Sub- and Supersonic Flow Conditions," 1996, AIAA 96-4566.
  37. Spirin, G.G., Vinogradov, Yu.K., Belyaev, O.V., "Experimental Study of Molecular Thermal Conductivity of Quartz," Teplofizika Vysokih Temperatur, v.34, No.1, 1996, p. 29.
  38. Dvurechensky, A.V., Petrov, V.A., Reznik, V.Yu., "Experimental Study of Quartz Glass Spectral Emissivity at High Temperatures," Teplofizika Vysokih Temperatur, v.16, No.4, 1978, p. 749.
  39. Petrov, V.A., Reznik, V.Yu., "Total Normal Emissivity of Quartz Glass of 'QR' Type at High Temperatures," Teplofizika Vysokih Temperatur, v.10, No.4, 1972, p. 778.
  40. Vasil'evskii, S.A., Kolesnikov, A.F., Yakushin, M.I., "Mathematical Models for Plasma and Gas Flows in Induction Plasmatrons," In: Molecular Physics and Hypersonic Flows, ed. by M.Capitelly, NATO ASI Series, v. 482, 1996, Kluwer, p. 495.
  41. Boulos, M.I., "The inductively coupled radio-frequency plasma," J. of Pure and Appl. Chem., 1985, v. 57, No. 9, p.1321.
  42. Kolesnikov, A.F., Vasil'evskii, S.A., "Some problems of numerical simulation of discharge electrodynamics in induction plasmatron," Proc. of 15th IMACS World Congress, Berlin, August 1997. v.3, Computational Physics, Chemistry and Biology. Ed. by A.Sydov, p.175.
  43. Kolesnikov, A.F., Vasil'evskii, S.A., "Results and Problems of Inductively Coupled Plasma Flows Modeling," IPM RAS, Preprint No. 610, Moscow 1998, 28 p.
  44. Patankar, S.V., Spalding, D.B., Heat and Mass Transfer in Boundary Layers. Intertext Books, London, 1970.
  45. Capitelli, M. and Devoto, R. S., "Transport Coefficients of High-Temperature Nitrogen," Phys. Fluids, 1973, v. 16, No. 11, p. 1835.
  46. Kolesnikov, A. F. and Tirkii, G. A., "Equations of Hydrodynamics for Partially Ionized Multi-Component Mixtures of Gases, Employing Higher Approximations of Transport coefficients," (tr. from Russian), in: Fluid Mechanics-Soviet Research, 1984, 1985 Scripta Technica, Inc., v. 13, No. 4, p. 70.
  47. Vanden Abeele, D., Vasil'evskii, S. A., Kolesnikov, A. F., Degrez, G., and Bottin, B., "Code-to-Code Validation of Inductive Plasma Computations," 1998, VKI, Reprint 1998-26.
  48. Vanden Abeele, D. and Degrez, G., "An Efficient Computational Model for Inductive Plasma Flows," 1998, AIAA 98-2825.
  49. Park, C., Candler, G.V., Howe, J.T., Jaffe, R.T., "Chemical-Kinetic Problems of Future NASA Missions," AIAA 91-0464.
  50. Kovalev, V.L., Suslov, O.N., Tirskiy, G.A., "Phenomenological Theory for Heterogeneous Recombination of Partially Dissociated Air on High Temperature Surfaces," In: Molecular Physics and Hypersonic Flows, ed. by M.Capitelly, NATO ASI Series, v. 482, 1996, Kluwer, p.193.
  51. Daiß, A., Frühauf, H.H., Messerschmid, E.W., "Chemical Reactions and Thermal Nonequilibrium on Silica Surfaces," In: Molecular Physics and Hypersonic Flows, ed. by M.Capitelly, NATO ASI Series, v. 482, 1996, Kluwer, p.203.
  52. Cacciatore, M., Rutigliano, M., and Billing, G. D., "Energy Flows, Recombination Coefficients and Dynamics for Oxygen Recombination on Silica Surfaces," 1998, AIAA 98-2843.
  53. Lin, S. Ch., and Teare, J. D., "Rate of Ionization behind Shock Waves in Air. II. Theoretical Interpretations," Phys. Fluids, 1963, v. 6, No. 3, p. 355.
  54. Vasil'evskii, S. A., Kolesnikov, A. F., and Yakushin, M. I., "Increased Heat Transfer to a Titanium Surface with Oxygen Injection into the Nonequilibrium Boundary Layer," Fluid Dynamics, Plenum, (tr. from Russian), 1991, v. 26, No. 4, p. 598.
  55. Greaves, J.C, Linnett, J.W., "Recombination of Oxygen Atoms on Silica from 20C to 600C," Trans. of the Faraday Society, 1955, v. 55, p.1355.
  56. Rubio Garcia, V., Marraffa, L., Scoon, G., Roumeas, R., "Mars Mini-Probes. Elements of Aerothermodynamics & Entry Trajectories," 3rd European Symposium on Aerothermodynamics for Space Vehicles, ESTEC, Noordwijk, The Netherlands, 24-26 November 1998, ESA SP-426, 1999, p. 155.